CELL CYCLE
2023, VOL. 22, NO. 18, 2038–2056
https://doi.org/10.1080/15384101.2023.2274670

Taylor & Francis
Taylor & Francis Group

RESEARCH PAPER

EIF4A3-regulated hsa_circ_0001445 can inhibit the progression of laryngeal squamous cell carcinoma via hsa-miR-432-5p-dependent up-regulation of RGMA expression

Miaomiao Yu, Huan Cao, Jianwang Yang, Tao Liu, Jiaxue Gao, and Baoshan Wang

Department of Otorhinolaryngology, The Second Hospital of Hebei Medical University, Shijiazhuang, China

ABSTRACT

Laryngeal squamous cell carcinoma (LSCC) is a common malignant tumor in the head and neck, the 5-year relative survival rate of patients diagnosed with laryngeal cancer was estimated to be 61% from 2012 to 2018. An increasing number of studies have shown that circular RNAs (circRNAs) play a key role in the occurrence and development of cancer and may function as cancer biomarkers and new therapeutic targets. At present, the research on the relationship between circRNAs and LSCC is still in its infancy and needs further exploration. In this study, we found a circRNA (hsa_circ_0001445) associated with LSCC based on bioinformatics analysis. Quantitative real-time polymerase chain reaction (qRT-PCR) assay indicated that the expression of hsa_circ_0001445 was down-regulated in LSCC tissues and cell lines. Notably, the expression of hsa_circ_0001445 was negatively correlated with aggressive clinicopathological features and poor prognosis. Then, functional experiments found that overexpression of hsa_circ_0001445 inhibited the proliferation, migration and invasion of LSCC cells and tumor growth in vivo. Mechanistically, RNA immunoprecipitation (RIP), biotin-labeled probe pull-down, luciferase reporter assay and western blot experiments were employed and found that EIF4A3 reduced the expression of hsa_circ_0001445, and the direct binding of hsa_circ_0001445 to hsa-miR-432-5p attenuated the inhibitory effect of hsa-miR-432-5p on RGMA. In summary, our research suggests that hsa_circ_0001445 may be used as a potential prognostic biomarker and therapeutic target for LSCC.

ARTICLE HISTORY
Received 21 August 2022
Revised 7 July 2023
Accepted 20 October 2023

KEYWORDS
Laryngeal squamous cell carcinoma; hsa_circ_0001445; hsa-miR-432-5p; RGMA; EIF4A3

Introduction

Laryngeal squamous cell carcinoma (LSCC) is a common malignant tumor in the head and neck, accounting for about 25% to 30% of all head and neck squamous cell cancers [1]. According to the latest global cancer statistics, there are 184615 new cases of laryngeal cancer and 99,840 deaths worldwide in 2020 [2]. The onset of laryngeal cancer is hidden, and most patients are at the advanced stages (clinical stages III and IV) at the time of diagnosis [3]. And laryngeal cancer is prone to local invasion and cervical lymph node metastasis [4]. Most of the treatment methods for laryngeal cancer are traditional methods, such as surgery, radiotherapy and chemotherapy, but the targeted therapy is very limited [5]. According to data from the Surveillance, Epidemiology, and End Results (SEER) Program, the 5-year relative survival rate of patients diagnosed with laryngeal cancer was estimated to be 61% from 2012 to 2018 [6]. Therefore, it is an urgent medical problem to explore the pathological mechanism of the occurrence and development of laryngeal cancer, look for potential prognostic biomarkers, and find ideal targets for molecular therapy.

Circular RNAs (circRNAs) are single-stranded closed-loop RNA molecules lacking poly adenylation (poly(A)) and capping [7]. Due to the rapid development of high-throughput sequencing technology, more and more differentially expressed circRNAs have been found in human normal and malignant cells [8]. And an increasing number of studies have shown that circRNAs play a key role in the occurrence and development of cancer and may function as cancer biomarkers and new therapeutic targets [9]. CircRNAs can act as microRNA (miRNA) sponges to perform regulatory roles. For instance, circALG1 was overexpressed in colorectal cancer and could promote the migration and invasion of CRC cells by sponging miR-342-5p to upregulate the expression

CONTACT Baoshan Wang hebwangbs@163.com Department of Otorhinolaryngology, The Second Hospital of Hebei Medical University, 215 Heping West Road, Shijiazhuang 050000, China
Supplemental data for this article can be accessed online at https://doi.org/10.1080/15384101.2023.2274670

of placental growth factor [10]. In addition, circRNAs can also bind to RNA binding proteins (RBPs) [11] and encode peptides [12].

At present, the research on the relationship between circRNAs and LSCC is still in its infancy. In this study, we found a circRNA (hsa_circ_0001445) associated with LSCC based on bioinformatics analysis. The expression of hsa_circ_0001445 was down-regulated in LSCC tissues and cell lines, and negatively correlated with aggressive clinicopathological features and poor prognosis. In addition, through a series of experiments, we proved that EIF4A3 reduced the expression of hsa_circ_0001445, and hsa_circ_0001445 inhibited the proliferation and metastasis of LSCC by directly binding to hsa-miR-432-5p to attenuate the inhibitory effect of hsa-miR-432-5p on RGMA. In summary, our research suggests that hsa_circ_0001445 may be used as a potential prognostic biomarker and therapeutic target for LSCC. We show the workflow of this study in Supplemental Figure 1.

Materials and methods

LSCC patient tissues

Tissue samples were collected from surgical patients in the Second Hospital of Hebei Medical University from 2016 to 2018, with a total of 57 pairs of LSCC tissues and matched adjacent non-tumor tissues. All patients did not receive chemotherapy or radiotherapy before operation. The study was approved by the Ethics Committee of the Second Hospital of Hebei Medical University. And all patients signed the informed consent forms. The tissue samples were independently diagnosed by two experienced clinical pathologists. Fresh specimens were immediately frozen in liquid nitrogen and stored at −80°C.

Cell lines and cell culture

Human LSCC cell lines (TU177 and AMC-HN-8), human nasopharyngeal epithelial cell line (NP69) and HEK293T cell line were stored in Biobank of Otorhinolaryngology Head and Neck Surgery of Hebei Medical University. TU177 cells were cultured in RPMI1640 medium (Gibco, Shanghai, China) containing 10% fetal bovine serum (FBS) (Lonsera, Uruguay). AMC-HN-8 and HEK293T cells were cultured in DMEM medium (Gibco, Shanghai, China) containing 10% FBS. NP69 was cultured in DMEM medium. All cells were cultured at 37°C with 5% CO_2.

RNA extraction, genomic DNA (gDNA) extraction and quantitative real-time polymerase chain reaction (qRT-PCR)

According to the manufacturer's instructions, total RNA was extracted from tissues or cells using RNA-easy Isolation Reagent (Vazyme, Nanjing, China). Nuclear and cytoplasmic RNA fractions were extracted using a PARIS™ Kit (Invitrogen, California, USA). Genomic DNA was extracted using DNA Extraction Reagent (Solarbio, Beijing, China). Reverse transcription was carried out with Transcriptor First Strand cDNA Synthesis Kit (Roche Diagnosis, Mannheim, Germany), and RNA was converted into cDNA. The detailed reverse transcription methods were shown in Supplemental Materials and Methods. QRT-PCR was performed with GoTaq®qPCR Master Mix (Promega, Wisconsin, USA). All primers were listed in Supplemental Table 1. CircRNA and mRNA expression were normalized by GAPDH or 18S rRNA, while U6 was used as the internal control for miRNA. Relative expression was normalized using the $2^{-\Delta\Delta Ct}$ method.

RNase R treatment

In the RNase R treatment experiment, total RNA (2ug) of TU177 and AMCHN-8 cells was incubated with or without 3 U/ug RNase R (Epicentre Technologies, Wisconsin, USA) at 37°C for 25 min and 70°C for 10 min. After that, the gDNA was removed and RT-PCR was carried out.

Cell transfection

The hsa_circ_0001445 overexpression plasmid was purchased from Hanbio (Shanghai, China). EIF4A3 and RGMA overexpression plasmid were purchased from Youbio (Changsha, China). RGMA siRNAs were synthesized by RiboBio (Shanghai, China). For luciferase reporter plasmids, the hsa_circ_0001445 sequence and RGMA 3′ untranslated region (3′ UTR) sequence of wild type or hsa-miR-432-5p binding site mutant were cloned into the pmirGLO vector

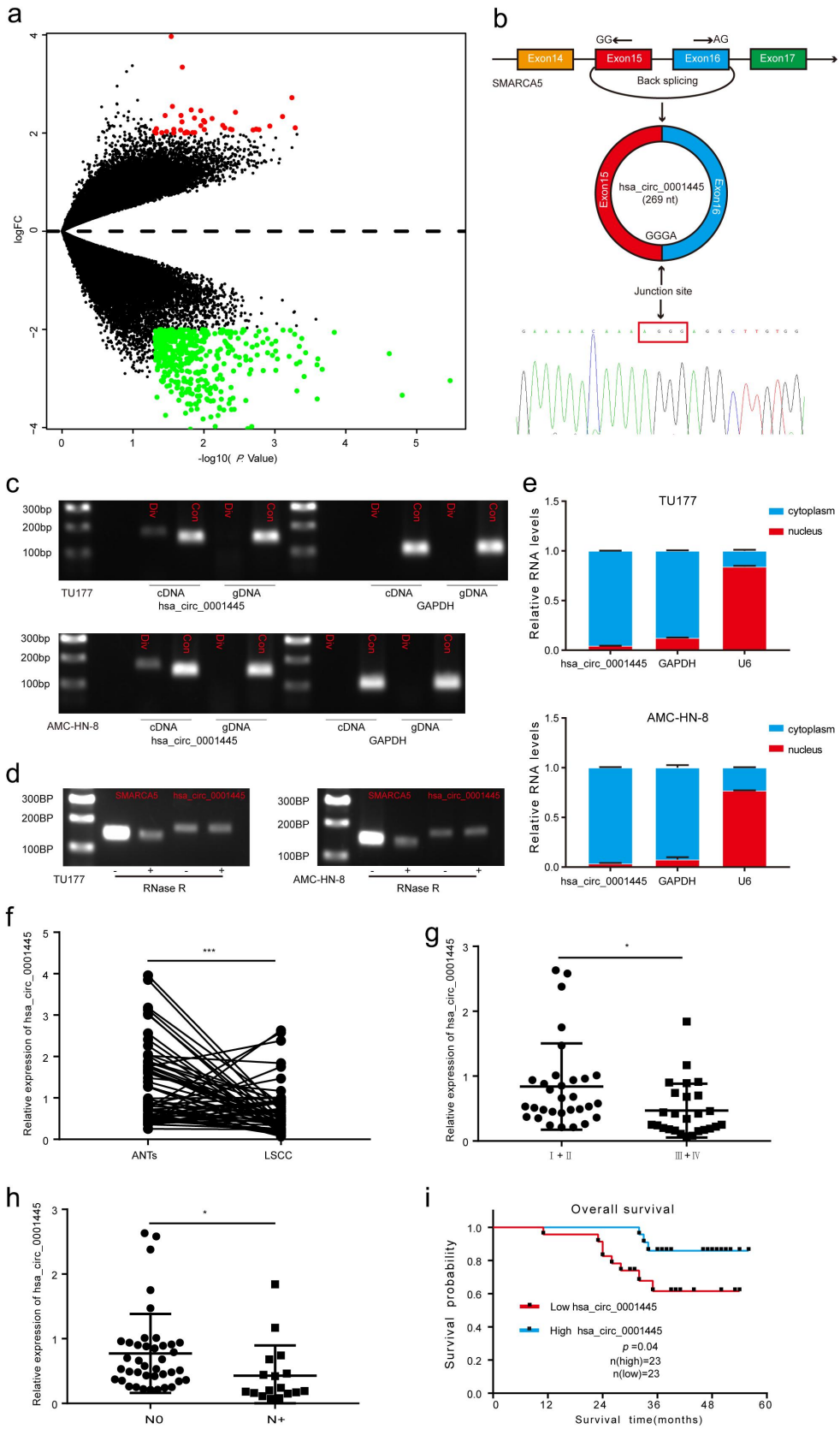

Figure 1. Identification and characteristics of hsa_circ_0001445 in LSCC and the expression of hsa_circ_0001445 in LSCC patients and its clinical significance.

(a) Volcano plot of the differentially expressed circRNAs in five pairs of LSCC tissues and matched adjacent non-tumor tissues. The red dots represent higher expression levels, while the green dots represent lower expression levels. (b) Schematic illustration showed the circularization of SMARCA5 exons 15 and 16 to form hsa_circ_0001445. Sanger sequencing following RT-PCR was used to show the "head-to-tail" splicing of hsa_circ_0001445. (c) Hsa_circ_0001445 expression in TU177 and AMC-HN-8 cells verified by RT-PCR.

(Youbio, Changsha, China). Hsa-miR-432-5p mimics and inhibitor were synthesized by RiboBio. According to the manufacturer's instructions, cells were transfected using Lipofectamine 2000 (Invitrogen, California, USA). All sequences were listed in Supplemental Table 1.

MTS assay

The proliferation ability of transfected TU177 and AMC-HN-8 cells was detected by MTS assay. After 48 h transfection, 2×10^3 cells/well were suspended in 100 μL medium containing 10% FBS and seeded into 96-well plate. According to the requirements of CellTiter 96® AQueous One Solution Cell Proliferation Assay Kit (Promega, Wisconsin, USA), 20 μL MTS/well was added into 96-well plate and incubated for 2 h. The absorbance values were measured at 490 nm wavelength by Spark® multimode microplate reader (Mod: SPARK 10 M, TECAN, Switzerland).

Colony formation assay

The transfected LSCC cells were seeded into a 6-well plate with a density of 2000 cells per well and cultured at 37°C for 10 days. Then, the cells were removed from the incubator, washed twice with PBS, fixed with 4% paraformaldehyde for 20 min, and stained with 0.1% crystal violet for 20 min. And then capture the image.

Transwell migration and invasion assays

LSCC cells transfected for 48 h were collected and suspended in serum-free medium. The cells were added to the upper chamber of transwell chamber (Corning, New York, USA) at a density of 1×10^5 cells per well, and 650 μL medium containing 10% FBS was added to the lower chamber. In the invasion assay, the transwell chambers were precoated with Matrigel (Corning, New York, USA). After 24 h, the cells in the upper chamber were wiped with cotton swabs, fixed with 4% paraformaldehyde for 20 min, and stained with 0.1% crystal violet for 20 min, and the images were collected under microscope.

RNA immunoprecipitation (RIP)

According to the specification of RNA Immunoprecipitation Kit (Geneseed Biotech, Guangzhou, China), the RIP assay was used to analyze the association of AGO2 with hsa_circ_0001445 and EIF4A3 with hsa_circ_0001445 flanking sequences. Briefly, 1×10^7 collected cells were added to 1 mL lysis buffer containing protease inhibitors and RNase inhibitors. The cell lysate was incubated overnight with protein A+G magnetic beads combined with FLAG antibody (#0912–1; HUABIO, Hangzhou, China), AGO2 antibody (#ab186733; Abcam, Cambridge, USA) or IgG (# HA1002; HUABIO, Hangzhou, China) at 4°C. After that, RNA and protein were separated. The obtained RNA was analyzed by qRT-PCR or RT-PCR, and the protein was analyzed by western blot analysis.

Biotin-labeled probe pull-down assay

In order to detect the interaction between hsa_circ_0001445 and miRNAs, a biotin-labeled probe pull-down assay was carried out according to the instructions of the CHIRP kit (Bersinbio, Guanzhou, China), with some modifications. About ^{7} 4×10cells were collected, lysed and sonicated. Then, the lysate was incubated with biotin-

Agarose gel electrophoresis showed that divergent primers amplified hsa_circ_0001445 in cDNA but not in gDNA. GAPDH served as a negative control. (d) Validation of hsa_circ_0001445 stability by RNase R treatment and RT-PCR assay. (e) Hsa_circ_0001445 abundance in nuclear and cytoplasmic fractions of TU177 and AMC-HN-8 cells was evaluated by qRT-PCR. GAPDH acted as a positive control of RNA distributed in the cytoplasm, and U6 RNA acted as a positive control of RNA distributed in the nucleus. (f) Expression levels of hsa_circ_0001445 in 57 paired LSCC tissues were determined by qRT-PCR. (g-h) The expression of hsa_circ_0001445 in different groups was evaluated according to the clinical features ($n_{(clinical\ stageI+II)} = 31$, $n_{(clinical\ stageIII+IV)} = 26$; $n_{(N0)} = 40$, $n_{(N+)} = 17$). I Kaplan-Meier analysis of the correlation between hsa_circ_0001445 expression and overall survival of 46 LSCC patients. Data represent means ± SD of three independent experiments. *$P< 0.05$, **$P< 0.01$, ***$P< 0.001$. Div, divergent primer; Con, convergent primer; ANTs, adjacent non-tumor tissues; N0, patients without cervical lymph node metastasis; N+, patients with cervical lymph node metastasis.

labeled probes (RiboBio Shanghai, China) at 37°C for 4 h. After that, the lysate -probes complex was incubated with streptavidin beads for 30 min. Finally, the magnetic beads were washed, and the RNA was extracted from the pull-down complex and analyzed by qRT-PCR. Probe sequences were listed in Supplemental Table 1.

Luciferase reporter assay

Luciferase reporter plasmid and hsa-miR-432-5p mimics or NC mimics were cotransfected into HEK293T cells for 48 h. Luciferase activity was measured with the Dual-Luciferase Reporter Assay System (Promega, Wisconsin, USA). The luciferase activities were expressed as the ratio of firefly luciferase to renilla luciferase activity.

Western blot analysis

Protein was extracted with RIPA lysis buffer containing PMSF (Solarbio, Beijing, China) and protease inhibitor cocktail (Promega, Wisconsin, USA). The protein concentration was determined using the BCA Protein Assay Kit (Generay, Shanghai, China). 20ug protein was separated by SDS-PAGE and transferred onto PVDF membranes (Bio-Rad, California, USA). The transferred membranes were blocked with 5% skim milk (Biofroxx, Einhausen, Germany) at room temperature for 2 h. The membranes were incubated with antibodies against FLAG (#0912–1, 1:5000; HUABIO, Hangzhou, China), EIF4A3 (#ET7108–11, 1:1000; HUABIO, Hangzhou, China), AGO2 (#ab186733,1:2000; Abcam, Cambridge, USA), RGMA (#HA500148, 1:2000; HUABIO, Hangzhou, China), ACTB (#-66009–1-Ig, 1:20000; Proteintech, Wuhan, China), or GAPDH (#10494–1-AP, 1:10000; Proteintech, Wuhan, China) overnight at 4°C. Then, membranes were washed three times with TBST followed by secondary antibody incubation for 2 h at room temperature. The band was detected by ChemiDoc™ XRS+ System (Bio-Rad, California, USA) with enhanced chemiluminescence (ECL) detection reagents (Vazyme, Nanjing, China).

Immunohistochemical (IHC) staining

The subcutaneous tumor tissues of nude mice were fixed with 4% paraformaldehyde, embedded in paraffin and cut into 4 μm sections. After dewaxing, rehydration, antigen retrieval and blocking, the sections were incubated with primary antibody (Ki67, AF1738, 1:150, Beyotime, Shanghai, China) overnight at 4°C. Then, Sections were incubated with the second antibody for 15 min at room temperature. DAB staining was performed for 1 min. Finally, the sections were stained with hematoxylin, dehydrated and sealed with a coverslip.

Generation of hsa_circ_0001445 overexpression cells and xenograft tumorigenesis

The lentivirus with overexpression of hsa_-circ_0001445 gene was purchased from Hanbio (Shanghai, China). Virus supernatant was mixed with polybrene and added to TU177 cells. After 72 h incubation, 2 μg/mL of puromycin was added for 48 h, and the stable cell clones were screened. SPF-grade male BALB/c nude mice (5–6 weeks) were purchased from Beijing HFK Bioscience Co., Ltd. (Beijing, China). Each mouse was subcutaneously injected into 200 μL serum-free medium containing 5×10^6 cells. The tumor volume was measured from the seventh day after injection. The tumor volume was calculated according to the following formula: $V(volume) = (length \times width^2)/2$. After 28 days, the mice were killed, dissected and weighed, and then histological analysis was performed. The study was approved by the Ethics Committee of the Second Hospital of Hebei Medical University.

Statistical analysis

SPSS 25.0, GraphPad Prism 7.0 and R (version 4.0.2) were used for statistical analysis. The two-tailed Student's t-test was used to compare the differences between the two groups. Kaplan-Meier survival curve and log-rank test were used to describe the overall survival probability of LSCC patients with different expression of hsa_circ_0001445. Hypergeometric test was used to test whether overlap is significant. The data was presented as mean ± standard deviation (SD). P values of < 0.05 were considered statistically significant.

Results

Identification and characteristics of hsa_circ_0001445 in LSCC

To identify the circRNAs associated with the progression of LSCC, we performed bioinformatics analysis based on a publicly available GEO data set (GSE117001) which included five pairs of LSCC tissues and matched adjacent non-tumor tissues. The analysis revealed a total of 352 significantly dysregulated circRNAs (|fold change| ≥ 4 and $P < 0.05$) and were presented in the volcano plot; 38 circRNAs were up-regulated, and 314 circRNAs were down-regulated (Figure 1a). Hsa_circ_0001445 (chr4:144464661–144465125) was generated from the SMARCA5 gene and consists of the head-to-tail splicing of exon 15–16 (269 bp) as reported in circBase. We designed a divergent primer to amplify the circular form of hsa_circ_0001445, and Sanger sequencing was used to confirm the existence of spliced junctions in hsa_circ_0001445 (Figure 1b). PCR and agarose gel electrophoresis assays showed that hsa_circ_0001445 could be amplified only in cDNA but not in gDNA (Figure 1c), eliminating artifacts caused by genomic rearrangement. Furthermore, we performed RNase R treatment assay to confirm the stability of hsa_circ_0001445. The results indicated that hsa_circ_0001445, but not linear SMARCA5 mRNA, was resistant to RNase R treatment (Figure 1d). Subsequently, nuclear-cytoplasmic fractionation assay was performed to detect the subcellular localization of hsa_circ_0001445. Through qRT-PCR after nuclear-cytoplasmic fractionation, we found that hsa_circ_0001445 was chiefly located in cytoplasm (Figure 1e). Taken together, these results revealed that hsa_circ_0001445, located in the cytoplasm, was a highly stable circRNA in LSCC.

Expression of hsa_circ_0001445 in LSCC patients and its clinical significance

To characterize the clinical significance of hsa_circ_0001445 in LSCC patients, we first verified its expression in 57 LSCC patients by qRT-PCR assay. The result indicated that hsa_circ_0001445 was significantly down-regulated in LSCC tissues compared with matched adjacent non-tumor tissues ($P < 0.001$) (Figure 1f). When we continued to explore the expression of hsa_circ_0001445 in tumor tissues, the results showed that the expression of hsa_circ_0001445 in stages III and IV was significantly lower than that in stage I and II (Figure 1g). And patients with cervical lymph node metastasis had lower expression levels of hsa_circ_0001445 (Figure 1h). In addition, Kaplan-Meier survival analysis based on the survival follow-up information of 46 patients suggested that patients with low expression of hsa_circ_0001445 had poor overall survival (Figure 1i). To sum up, these results suggest that the expression of hsa_circ_0001445 was significantly down-regulated in LSCC tissues, and the decreased expression of hsa_circ_0001445 may indicate poor prognosis.

Hsa_circ_0001445 inhibits proliferation, migration and invasion of LSCC cells in vitro

In order to explore the function of hsa_circ_0001445, we detected the expression of hsa_circ_0001445 in human LSCC cell lines (TU177 and AMC-HN-8) and human nasopharyngeal epithelial cell line (NP69). We found the expression of hsa_circ_0001445 was significantly down-regulated in LSCC cells (Figure 2a). We constructed one overexpression plasmid of hsa_circ_0001445 and transfected it into LSCC cells (TU177 and AMC-HN-8), which successfully increased the expression of hsa_circ_0001445 but not SMARCA5 mRNA as confirmed by qRT-PCR analysis (Figure 2b). According to the MTS assay, we found that overexpression of hsa_circ_0001445 significantly inhibited the viability of TU177 and AMC-HN-8 cells (Figure 2c). In addition, colony formation assay revealed that the prolifetation of TU177 and AMC-HN-8 cells in hsa_circ_0001445 up-regulated group was also repressed compared with negative control group (Figure 2d). Furthermore, the effect of hsa_circ_0001445 on the migration and invasion of LSCC cells was detected by transwell assay. The results showed that the up-regulation of hsa_circ_0001445 expression remarkably suppressed the migration and invasion of TU177 and AMC-HN-8 cells (Figure 2e-f). In conclusion, these results demonstrated that hsa_circ_0001445 acted as a tumor suppressor gene in LSCC.

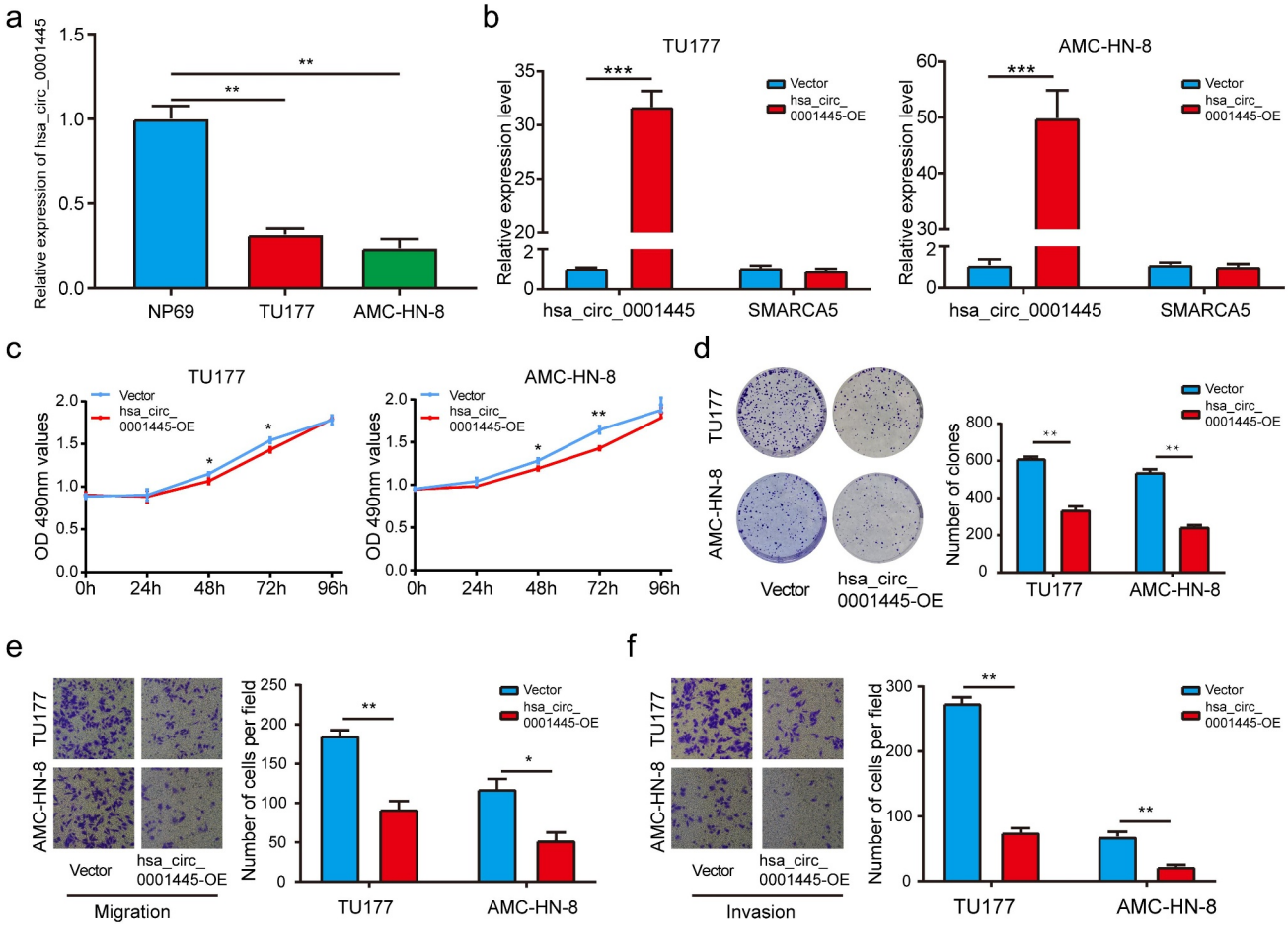

Figure 2. Hsa_circ_0001445 inhibits proliferation, migration and invasion of LSCC cells in vitro.

(a) QRT-PCR analysis of the hsa_circ_0001445 expression in human LSCC cell lines (TU177 and AMC-HN-8) and human nasopharyngeal epithelial cell line (NP69). (b) One overexpression plasmid of hsa_circ_0001445 was transfected into LSCC cells (TU177 and AMC-HN-8), and the expression levels of hsa_circ_0001445 and SMARCA5 were detected by qRT-PCR. (c) The effect of hsa_circ_0001445 on cell proliferation in TU177 and AMC-HN-8 cells was detected by MTS assay. (d) Hsa_circ_0001445 overexpression inhibited colony formation of both TU177 and AMC-HN-8 cells. (e) & (f) The cell migration and invasion ability of TU177 and AMC-HN-8 cells after overexpression of hsa_circ_0001445 were examined by transwell assay. Data represent means ± SD of three independent experiments. *P< 0.05, **P< 0.01, ***P< 0.001.

EIF4A3 suppresses the expression of hsa_circ_0001445 in LSCC

To explore the reason for the differential expression of hsa_circ_0001445 in LSCC, we used Circular RNA Interactome (https://circinteractome.nia.nih.gov/) to predict RBP sites that match the flanking regions of hsa_circ_0001445. As show in Figure 3a, EIF4A3 has six binding sites. We divided the six binding sites into three parts, which were named as a, b and c. RIP assay was used to verify the binding of EIF4A3 with putative binding sites. The results indicated that EIF4A3 can bind with linear RNA through two putative binding sites, which we named a and c, but not b (Figure 3b). In order to determine the role of EIF4A3 in hsa_circ_0001445 cyclization, we first analyzed the expression of EIF4A3 in head and neck squamous cell carcinoma through GEPIA database. Although there is no significant overexpression of EIF4A3 in tumor tissues compared with the corresponding normal tissues, the survival time of patients with high expression of EIF4A3 is shorter than that of patients with low expression of EIF4A3 (Figure 3c). Next, we examined the expression level of hsa_circ_0001445 in cells with EIF4A3 overexpression. The results showed that the expression of hsa_circ_0001445 was markedly downregulated in EIF4A3

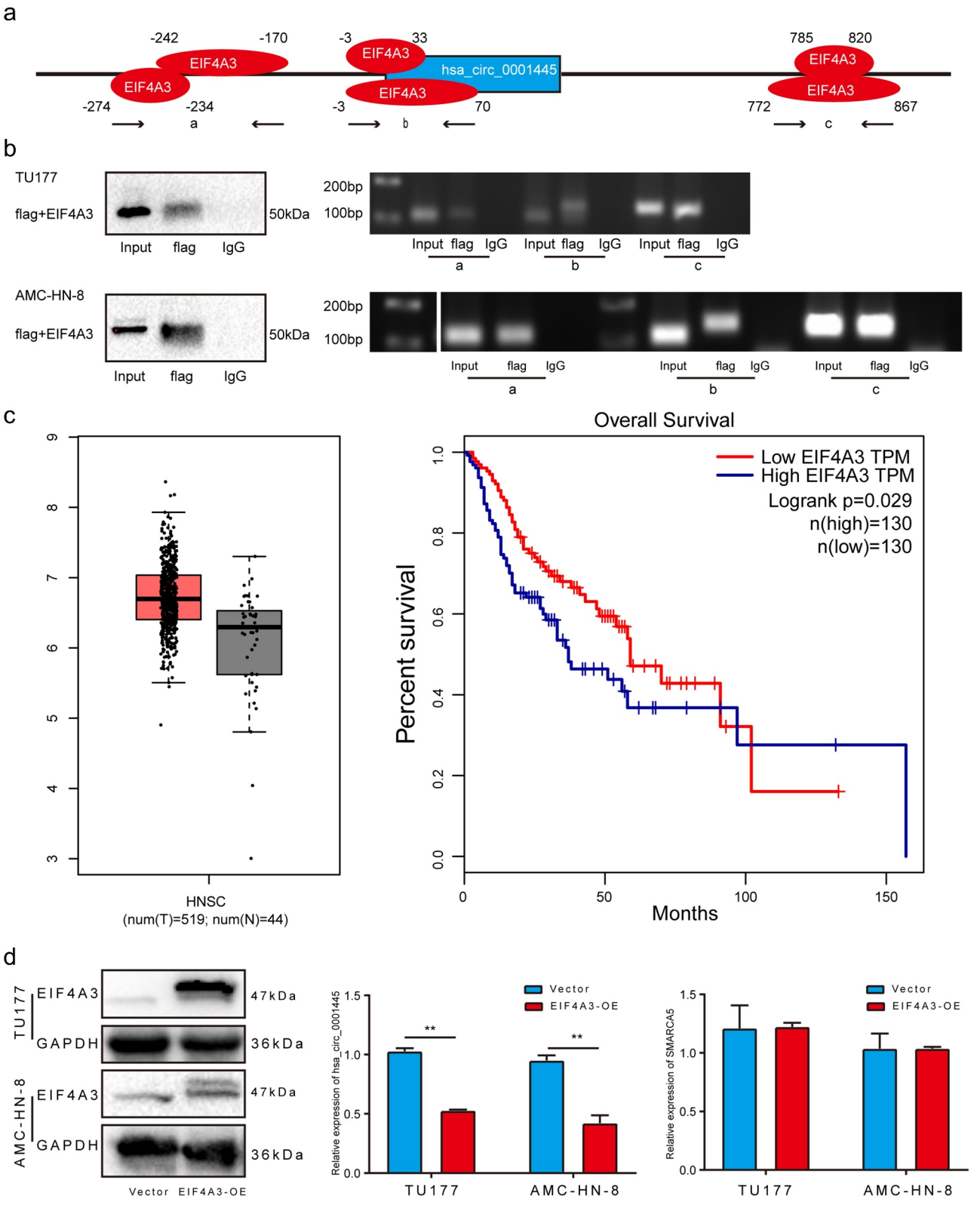

Figure 3. EIF4A3 suppresses the expression of hsa_circ_0001445 in LSCC.

(a) The diagram shows the binding sites of EIF4A3 on the flanking region of hsa_circ_0001445 predicted by Circular RNA Interactome. (b) The RIP assay was performed to verify the binding sites of EIF4A3 on the flanking region of hsa_circ_0001445. (c) Using GEPIA to analyze the expression of EIF4A3 in head and neck squamous cell carcinoma and its effect on patients' survival. (d) Western blot analysis was used to verify the successful overexpression of EIF4A3 in LSCC cells, and qRT-PCR was used to detect the expression of hsa_circ_0001445 and SMARCA5 after overexpression of EIF4A3. Data represent means ± SD of three independent experiments. *P< 0.05, **P< 0.01, ***P< 0.001.

overexpression cells (Figure 3d). In summary, these data suggested that EIF4A3 reduced the expression of hsa_circ_0001445 by binding to flanking sequences.

Hsa_circ_0001445 acts as a sponge for hsa-miR-432-5p in LSCC

According to the literature, circRNAs located in the cytoplasm usually act as miRNA sponges to regulate the expression of downstream target genes. We first explored whether hsa_circ_0001445 had the function of binding to miRNAs. Through RIP assay, we found that hsa_circ_0001445 could be amplified from the immunoprecipitate of AGO2 antibody group, indicating that hsa_circ_0001445 might have the function of binding to miRNAs (Figure 4a). In order to further identify the miRNAs binding to hsa_circ_0001445 in LSCC, we conducted a cross-analysis using two online databases: Circular RNA Interactome and Starbase 3.0. Two miRNAs (hsa-miR-579-3p, hsa-miR-432-5p) were found to be potential targets for hsa_circ_0001445 (Figure 4b). Next, we designed a biotin-labeled hsa_circ_0001445 probe and a negative control probe for RNA pull-down assay, and qRT-PCR verified the effectiveness of the probes. Two potential miRNAs were tested in pull-down fraction by qRT-PCR assay. The enrichment of hsa-miR-432-5p in the hsa_circ_0001445 pull-down fraction was significantly higher than negative control group. But there was no significant difference in the enrichment of hsa-miR-579-3p between hsa_circ_0001445 pull-down fraction and negative control group (Figure 4c). In order to elucidate the interaction between hsa_circ_0001445 and hsa-miR-432-5p, we inserted the wild type or mutant hsa_circ_0001445 sequence of hsa-miR-432-5p binding site into pmirGLO vector for luciferase reporter assay. The results showed that the transfection of hsa-miR-432-5p mimics significantly inhibited the luciferase activity in the cells expressing hsa_circ_0001445 wild-type reporter gene, but there was no significant effect on luciferase activity in the cells expressing hsa_circ_0001445 mutant reporter gene (Figure 4d). In general, hsa_circ_0001445 might play the role of ceRNA by targeting hsa-miR-432-5p in LSCC.

Hsa-miR-432-5p is upregulated in LSCC and acts as a oncogene by targeting RGMA

Due to the interaction between hsa_circ_0001445 and hsa-miR-432-5p, we first verified the expression level of hsa-miR-432-5p in 26 LSCC patients by qRT-PCR assay. The results showed that compared with matched adjacent non-tumor tissues, hsa-miR-432-5p was significantly up-regulated in LSCC tissues ($p < 0.05$) (Figure 5a). In order to evaluate the function of hsa-miR-432-5p, we transfected a miRNA inhibitor or control construct into TU177 cells and AMC-HN-8 cells, and carried out MTS assay, clone formation assay and transwell assay. The results showed that compared with the control group, the proliferation, migration and invasion of LSCC cells transfected with hsa-miR-432-5p inhibitor were significantly inhibited (Figure 5b-e).

In order to further identify the downstream target genes of hsa-miR-432-5p, we used two databases (TargetScan 8.0 and starbase3.0) to predict, performed RNA-seq after overexpressing hsa_circ_0001445, and analyzed the low expression genes of LSCC in TCGA database. After further reading the literature, we found that RGMA may be the target gene of hsa-miR-432-5p in LSCC. And then, we conducted luciferase reporter assay. The results showed that hsa-miR-432-5p mimics significantly inhibited the luciferase activity in the cells expressing RGMA wild-type reporter gene, but there was no significant effect on luciferase activity in the cells expressing RGMA mutant reporter gene (Figure 5f). The effect of hsa-miR-432-5p on RGMA was further verified by qRT-PCR and western blot analysis. The results showed that the mRNA and protein expression level of RGMA in hsa-miR-432-5p inhibitor group were significantly higher than that in control group (Figure 5g). Previous studies have shown that RGMA plays a tumor suppressor gene role in gallbladder carcinoma [13], breast cancer [14] and oral squamous cell carcinoma [15], but no one has studied the biological role of RGMA in LSCC. In this study, when we transfected RGMA overexpression plasmid into TU177 cells and AMC-HN-8 cells, we found that cell proliferation, migration and invasion were significantly inhibited compared with the control group (Figure 5h-i). In conclusion, these results suggested that RGMA acted as a tumor suppressor gene in LSCC, and hsa-miR-432-5p promotes the

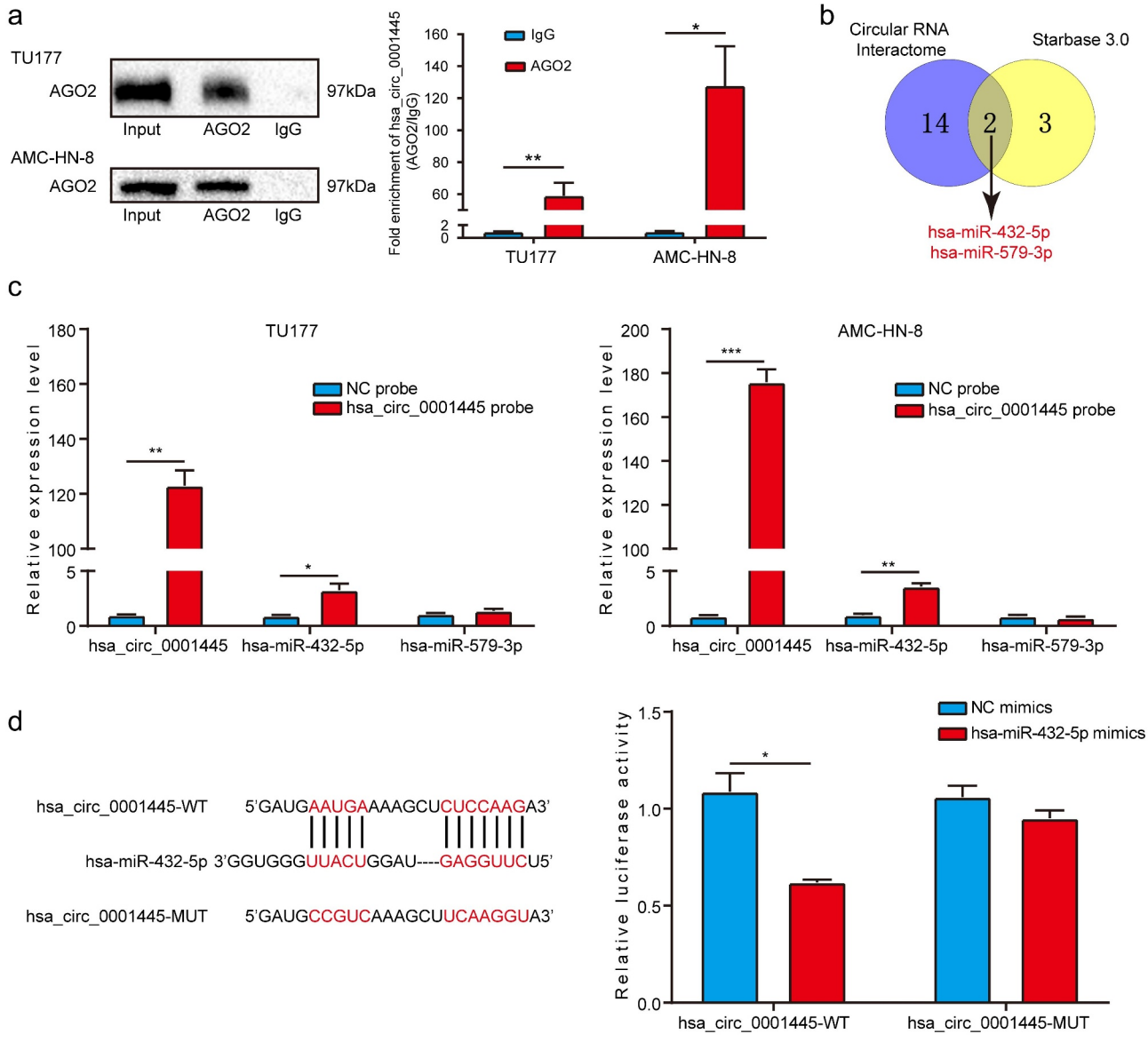

Figure 4. Hsa_circ_0001445 acts as a sponge for hsa-miR-432-5p in LSCC.

(a) RIP assay was carried out with AGO2 antibody in TU177 and AMC-HN-8 cells, and then the enrichment of hsa_circ_0001445 was detected by qRT-PCR. (b) Combined analysis of two online databases (Circular RNA Interactome and Starbase 3.0) to screen for hsa_circ_0001445-binding miRNAs, $p = 1.782164e\text{-}06$. (c) Relative level of hsa_circ_0001445 in TU177 and AMC-HN-8 lysates after RNA pull down using hsa_circ_0001445 probe or NC probe. And relative level of two miRNAs in TU177 and AMC-HN-8 lysates pulled down by hsa_circ_0001445 probe or NC probe. (d) HEK293T cells were co-transfected with hsa-miR-432-5p mimics and wild-type (hsa_circ_0001445-WT) or mutant (hsa_circ_0001445-MUT) hsa_circ_0001445 luciferase reporter vector, and luciferase activity was detected. Data represent means ± SD of three independent experiments. *P< 0.05, **P< 0.01, ***P< 0.001. NC, negative control.

proliferation, migration and invasion of LSCC by targeting RGMA.

Hsa_circ_0001445 attenuates the tumor-promoting effect of hsa-miR-432-5p on LSCC cells

We cotransfected hsa_circ_0001445 overexpression plasmid and hsa-miR-432-5p mimics into LSCC cells to carry out rescue experiments. The results indicated that compared with the cells transfected only with hsa-miR-432-5p mimics, up-regulation of hsa_circ_0001445 could attenuate the enhancement of proliferation, migration and invasion abilities induced by hsa-miR-432-5p minics in TU177 and AMC-HN-8 cells (Figure 6a-d). In addition, the mRNA and protein expression level of RGMA were detected by qRT-PCR and western blot analysis. The

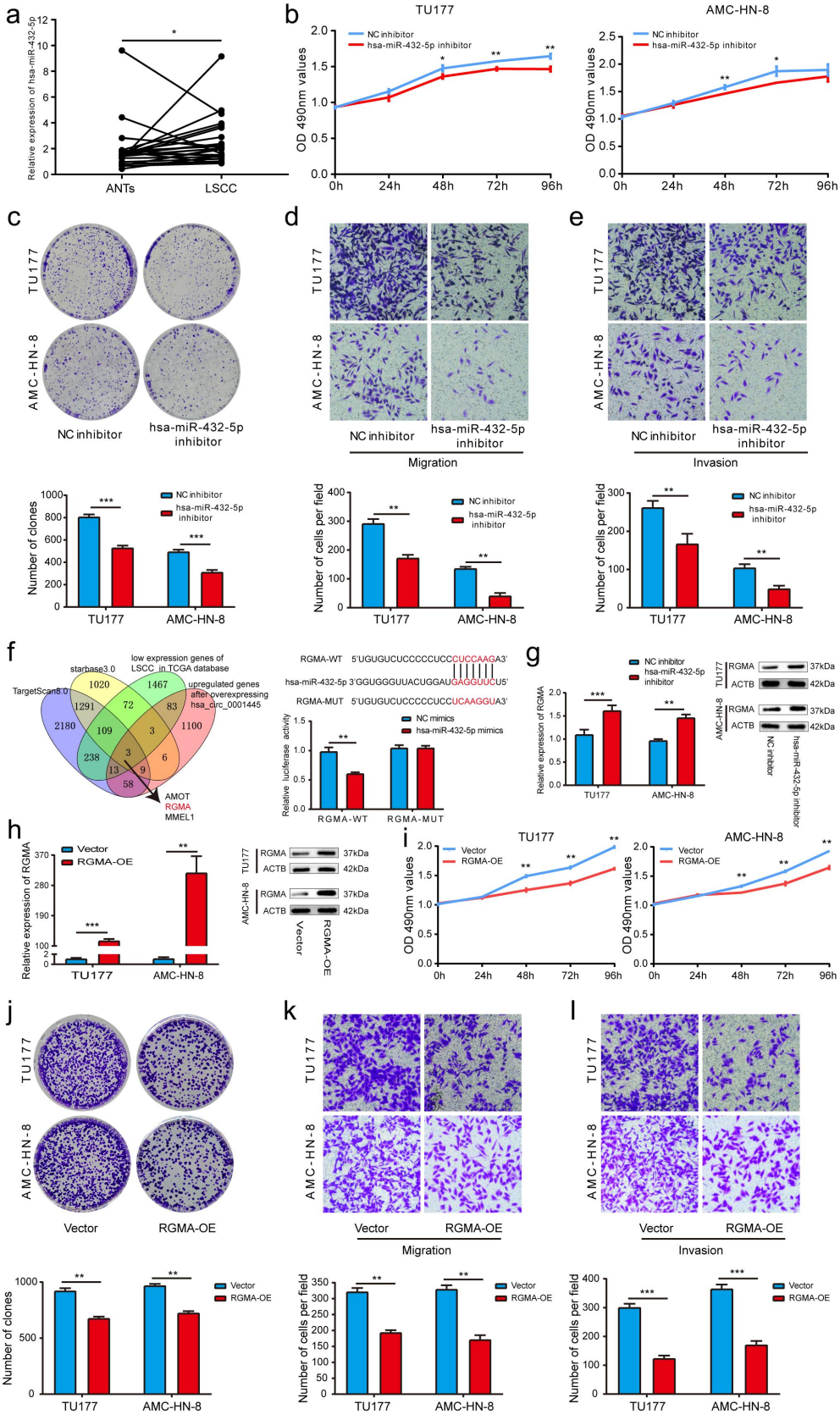

Figure 5. Hsa-miR-432-5p is upregulated in LSCC and acts as a oncogene by targeting RGMA.

(a) Expression levels of hsa-miR-432-5p in 26 paired LSCC tissues were determined by qRT-PCR. (b) The effect of hsa-miR-432-5p on cell proliferation in TU177 and AMC-HN-8 cells was detected by MTS assay. (c) Hsa-miR-432-5p inhibitor inhibited colony formation of both TU177 and AMC-HN-8 cells. (d & e) The cell migration and invasion ability of TU177 and AMC-HN-8 cells after hsa-miR-432-5p

results showed that compared with the LSCC cells transfected only with hsa-miR-432-5p mimics, the mRNA and protein expression level of RGMA of LSCC cells cotransfected with hsa_circ_0001445 overexpression plasmid and hsa-miR-432-5p mimics were increased (Figure 6e-f). Taken together, these results suggested that hsa_circ_0001445 inhibited the progression of LSCC cells partly by weakening the tumor promoting the effect of hsa-miR-432-5p.

Silencing RGMA attenuates the inhibitory effect of hsa_circ_0001445 on LSCC cells

In order to further study whether hsa_circ_0001445 exerts its inhibitory effect on LSCC cells by inducing the expression of RGMA, we carried out rescue experiments to detect the functional interaction between hsa_circ_0001445 and RGMA. The results showed that knockdown of RGMA gene could attenuate the inhibition of hsa_circ_0001445 overexpression on the proliferation, migration and invasion of TU177 and AMC-HN-8 cells compared with the cells transfected only with hsa_circ_0001445 overexpression plasmid (Figure 7a-e). Collectively, these results demonstrated that hsa_circ_0001445 exerted its inhibitory effect on LSCC by inducing the expression of RGMA.

Hsa_circ_0001445 inhibits tumor growth in vivo

In order to study the regulatory effect of hsa_circ_0001445 on LSCC in vivo, we constructed xenograft tumor models of nude mice by subcutaneously injecting TU177 cells stably overexpressing hsa_circ_0001445 or contral cells. The volume of xenograft tumors formed by hsa_circ_0001445 overexpressing LSCC cells was significantly smaller than that in the control group (Figure 8a), and the tumor weight was also significantly lower than that in the control group (Figure 8b). In addition, IHC staining demonstrated that the expression of Ki67, a proliferation marker, was decreased in xenograft tumors with overexpression of hsa_circ_0001445 (Figure 8c). These results confirmed that hsa_circ_0001445 inhibited the proliferation of LSCC in vivo.

Discussion

Previous studies have shown that circRNAs play an important regulatory role in a variety of biological processes, especially in the occurrence and development of various malignant tumors [16–18]. In this study, we found a circRNA (hsa_circ_0001445) associated with LSCC based on bioinformatics analysis, and the expression of hsa_circ_0001445 in LSCC was significantly down-regulated. We further searched the database and verified by experiments that hsa_circ_0001445 was a circular RNA composed of exons 15 and 16 of SMARCA5. CircRNAs are highly stable because they are resistant to RNA exonuclease or RNase R [19]. After treatment with RNase R, the expression of hsa_circ_0001445 did not change significantly, which was consistent with the previous report that circRNAs have high stability. Importantly, we found that the low expression of hsa_circ_0001445 was associated with the advanced clinical stage and poor prognosis of LSCC, suggesting that hsa_circ_0001445 might play an important role in the occurrence and development of LSCC.

Previous study has shown that CircRNA_ACAP2 suppresses EMT in head and neck squamous cell carcinoma [20]. Gao et al. confirmed that CircPARD3 leads to malignant progression and chemotherapy resistance of LSCC by inhibiting autophagy [21]. circCUX1 promotes radiotherapy resistance of hypopharyngeal squamous cell carcinoma [22]. And circIGHG

knockdown were examined by transwell assay. (f) Combined analysis to screen for hsa-miR-432-5p-binding mRNAs. The hsa-miR-432-5p mimics and wild type (RGMA-WT) or mutant (RGMA-MUT) RGMA-luciferase reporter vector were cotransfected into HEK293T cells, and the luciferase activity was detected. (g) The effect of hsa-miR-432-5p on RGMA was verified by qRT-PCR and western blot analysis. (h) QRT-PCR and western blot analysis were used to verify the successful overexpression of RGMA in LSCC cells. (i) The effect of RGMA on cell proliferation in TU177 and AMC-HN-8 cells was detected by MTS assay. (j) RGMA overexpression inhibited colony formation of both TU177 and AMC-HN-8 cells. (k & L) The cell migration and invasion ability of TU177 and AMC-HN-8 cells after overexpression of RGMA were examined by transwell assay. Data represent means ± SD of three independent experiments. *$P< 0.05$, **$P< 0.01$, ***$P< 0.001$.

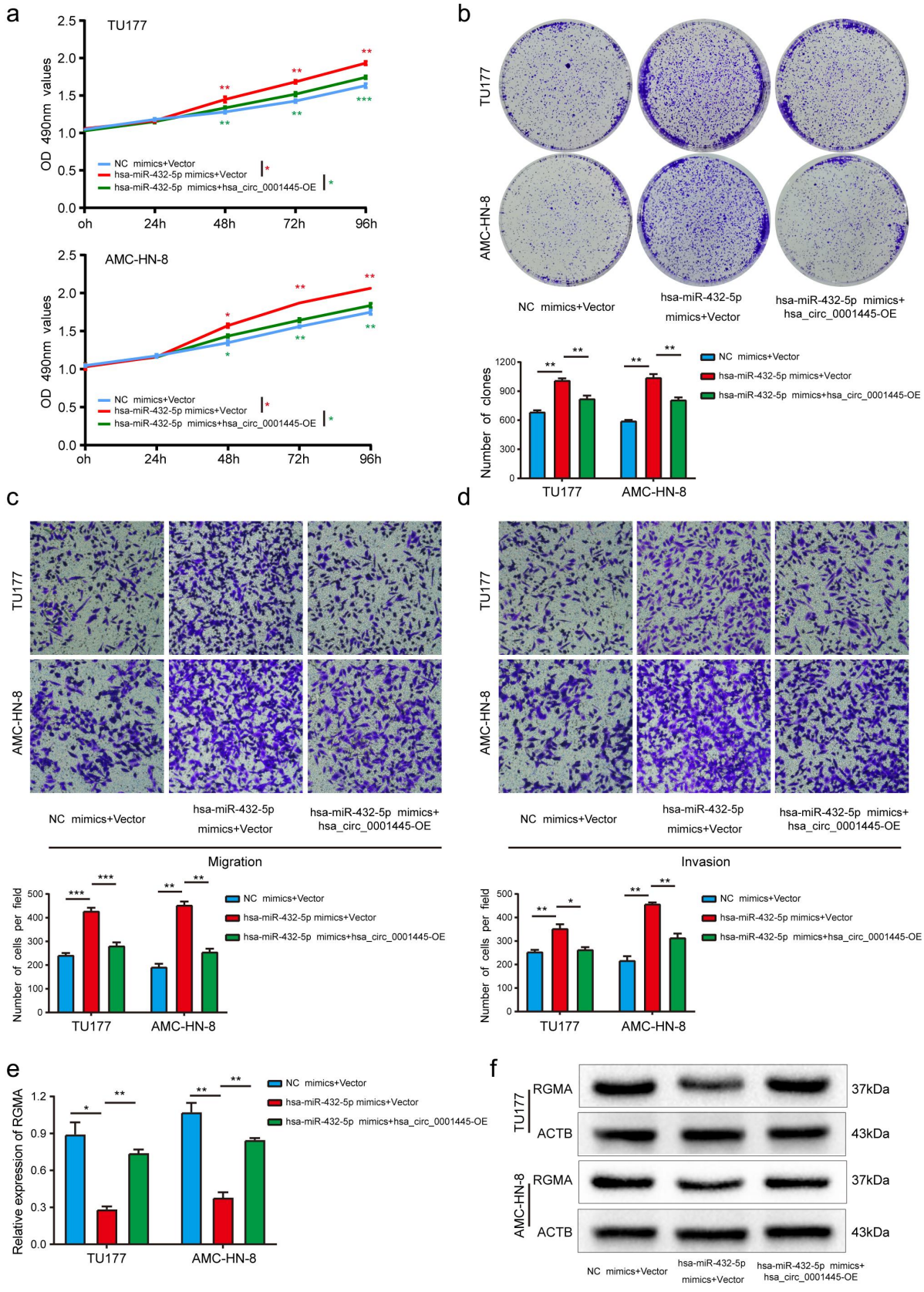

Figure 6. Hsa_circ_0001445 attenuates the tumor-promoting effect of hsa-miR-432-5p on LSCC cells.

(a & b) MTS and colony formation assays indicated that the cell proliferation ability of TU177 and AMC-HN-8 cells transfected with hsa-miR-432-5p mimics was reversed when co-transfected with overexpression plasmid of hsa_circ_0001445. (c & d) Transwell assay demonstrated that cell migration and invasion abilities of TU177 and AMC-HN-8 cells transfected with hsa-miR-432-5p mimics were

promotes the proliferation, migration and invasion of oral squamous cell carcinoma [23]. In addition, previous studies have shown that hsa_circ_0001445 inhibits the malignant progression of hepatocellular carcinoma [24] and glioblastoma multiforme [25], but plays a role as an oncogene in osteosarcoma [26]. In this study, we explored the role of hsa_circ_0001445 in LSCC. The results showed that overexpression of hsa_circ_0001445 inhibited the proliferation, migration and invasion of LSCC cells, indicating that hsa_circ_0001445 was an important tumor suppressor gene that inhibited the malignant progression of LSCC.

Previous studies have shown that some RNA binding proteins can promote or inhibit the formation of circRNAs. For example, QKI promotes the formation of circRNA by binding to flanking intron sequences [27]. It is reported that FUS is also a regulator of circRNAs formation [28,29]. In addition, it is reported that ADAR1 destroys the stability of double-stranded RNA in the flanking intron through A-to-I editing, thus inhibiting the biogenesis of circRNAs [30]. However, the function and potential mechanism of most RBP in regulating the formation of circRNAs are still unclear. In this study, we found that EIF4A3 could bind to the flanking region of hsa_circ_0001445 and inhibit its expression. Previous studies have shown that EIF4A3 inhibited circPTEN1 formation in colorectal cancer [31], circRNA_100290 in gastric cancer [32], and circ_0087429 in cervical cancer [33]. However, in prostate cancer, EIF4A3 promoted the formation of circARHGAP29 and in hepatocellular carcinoma, EIF4A3 promoted the formation of circTOLLIP [34,35]. (Figure 8d) This suggests that the effect of EIF4A3 on the formation of circRNAs may be related to the type of cancer, although the underlying mechanism is not clear.

The competitive endogenous RNA (ceRNA) hypothesis proposes a mechanism, that is, lncRNAs, circRNAs and mRNAs affect the stability or translation of the target RNAs through competitively binding to the same miRNAs [36]. In this study, we proved that hsa_circ_0001445 was mainly located in the cytoplasm through nuclear-cytoplasmic fractionation assay. This suggested that hsa_circ_0001445 may play a role through ceRNA mechanism [37]. Through bioinformatics prediction and a series of experiments, we found that hsa_circ_0001445 acts as a sponge of hsa-miR-432-5p. Studies have shown that hsa-miR-432-5p, as an oncogene, affects the malignant progression of bladder cancer [38] but plays a role of tumor suppressor gene in colorectal cancer [39]. In this study, we verified that the expression of hsa-miR-432-5p in LSCC tissues was significantly up-regulated compared with matched adjacent non-tumor tissues, and hsa-miR-432-5p inhibitor could significantly inhibit the proliferation, migration and invasion of LSCC cells. We further looked for the downstream target gene of hsa-miR-432-5p and found that hsa-miR-432-5p may affect the stability of RGMA and reduce its expression in LSCC. RGMA acts as a tumor suppressor gene in a variety of tumors. For example, in gallbladder cancer, overexpression of RGMA inhibited cell proliferation and migration [13]. In breast cancer, RGMA overexpression markedly inhibited the migration and invasion capabilities of tumor cells [14]. In oral squamous cell carcinoma, the ectopic expression of RGMA significantly inhibited the proliferation of OSCC cells both in vitro and in vivo [15]. (Figure 8d) Functional studies showed that the overexpression of RGMA inhibited the proliferation, migration and invasion of LSCC cells. Through rescue experiments, we found that the overexpression of hsa_circ_0001445 could partially reverse the inhibitory effect of hsa-miR-432-5p mimics on RGMA and weaken the promoting effect of hsa-miR-432-5p on malignant phenotype of LSCC. Knockdown of RGMA gene could attenuate the inhibition of hsa_circ_0001445 overexpression on the proliferation, migration and invasion of LSCC. Therefore, we confirmed that the competitive binding of hsa_circ_0001445 and

counteracted when co-transfected with overexpression plasmid of hsa_circ_0001445. (e & f) QRT-PCR and western blot assays demonstrated that hsa_circ_0001445 could counteract the influence of hsa-miR-432-5p mimics on RGMA expression in LSCC cells. Data represent means ± SD of three independent experiments. *$P< 0.05$, **$P< 0.01$, ***$P< 0.001$.

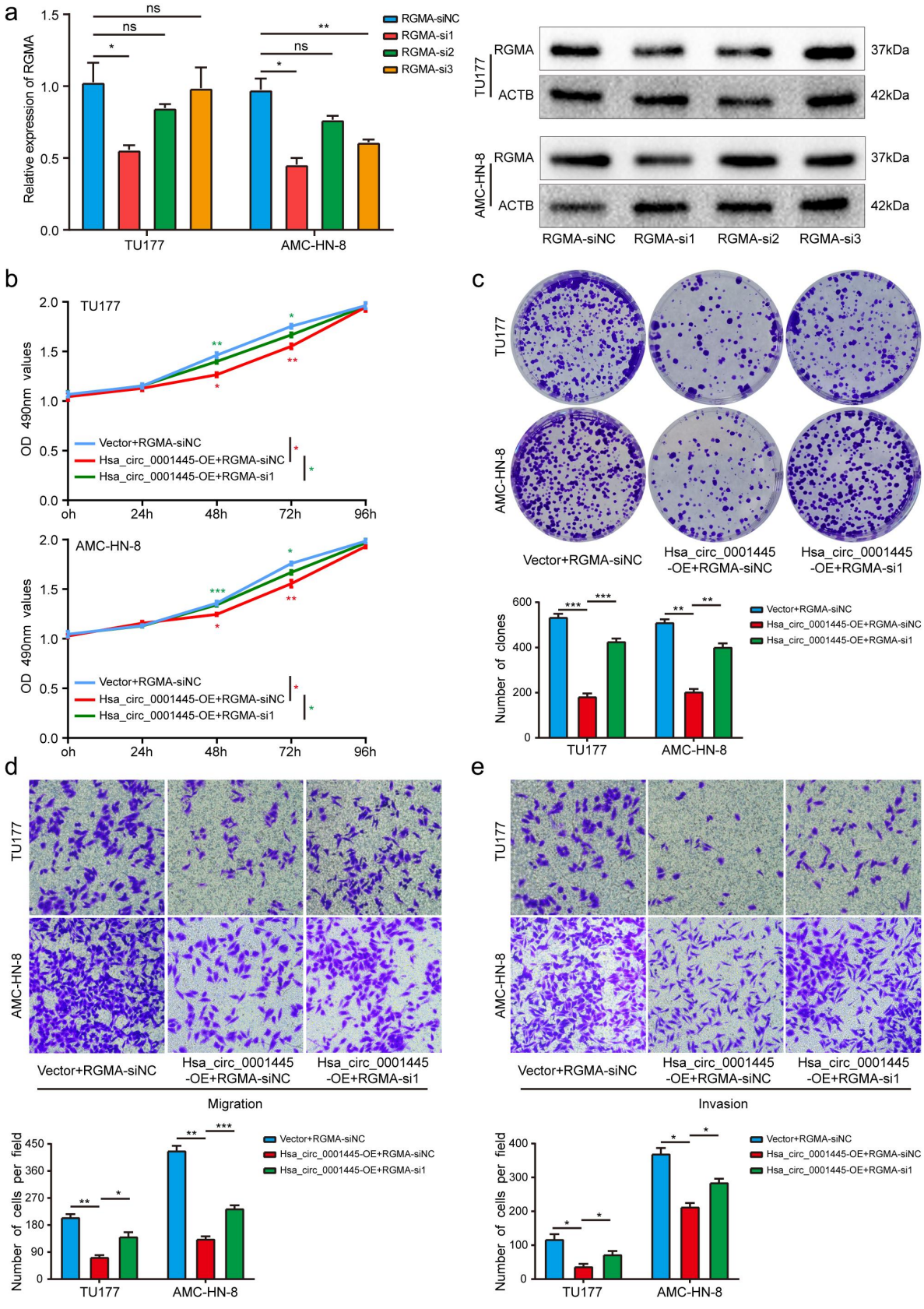

Figure 7. Silencing RGMA attenuates the inhibitory effect of hsa_circ_0001445 on LSCC cells.

(a) QRT-PCR and western blot analysis were used to verify the successful knockdown of RGMA in LSCC cells. (b) & (c) MTS and colony formation assays indicated that cell proliferation ability of TU177 and AMC-HN-8 cells transfected with overexpression plasmid of hsa_circ_0001445 was reversed when co-transfected with RGMA siRNA. (d & e) Transwell assays demonstrated that cell migration and invasion abilities of TU177 and AMC-HN-8 cells transfected with overexpression plasmid of hsa_circ_0001445 were counteracted when co-transfected with RGMA siRNA. Data represent means ± SD of three independent experiments. *P< 0.05, **P< 0.01, ***P< 0.001.

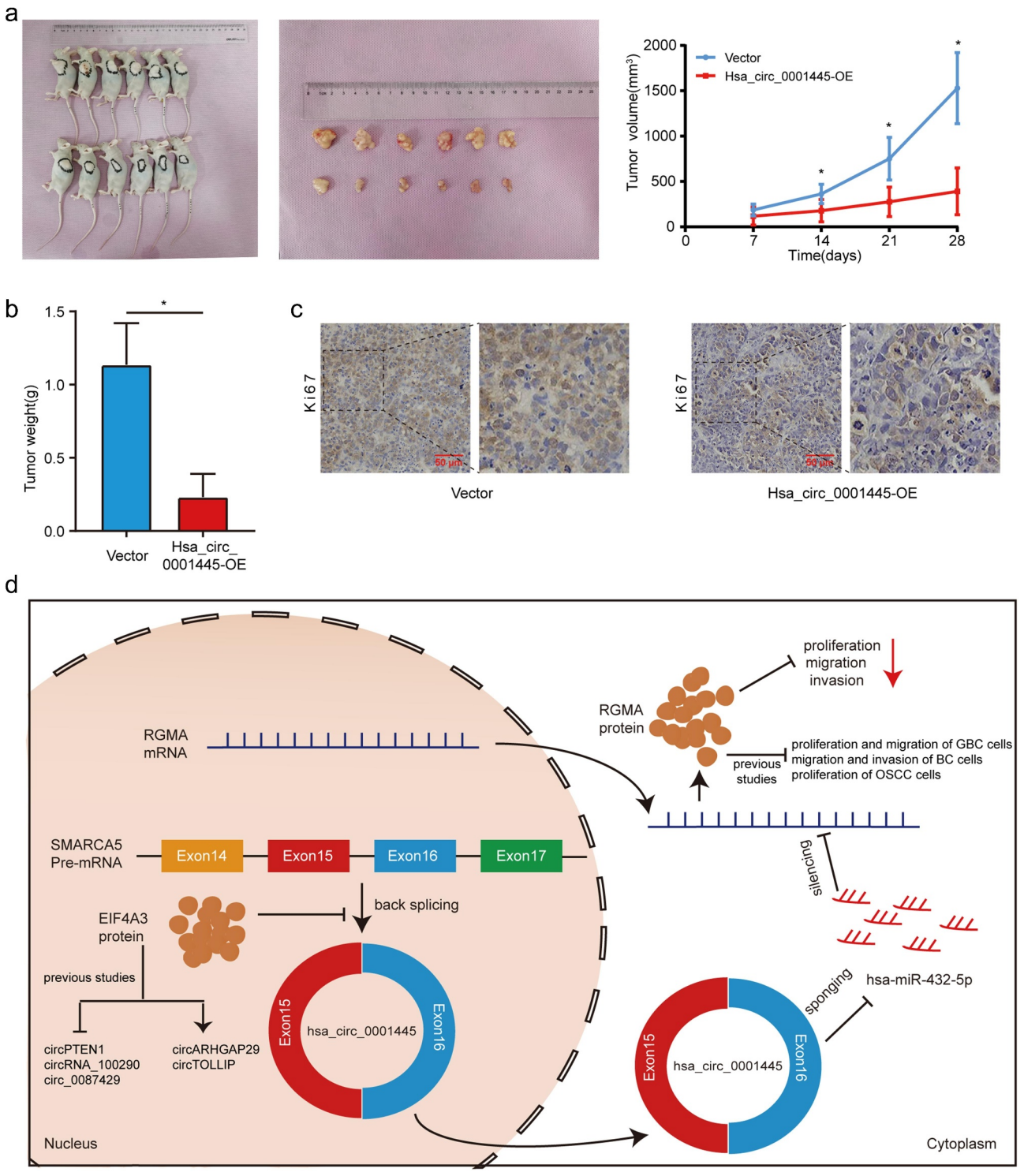

Figure 8. Hsa_circ_0001445 inhibits tumor growth in vivo.

(a) Images of xenograft tumors in nude mice. And comparison of the tumor volume in hsa_circ_0001445-OE and vector group. Data represents mean ± SD ($n = 6$ each group), *$P < 0.05$. (b) Tumor weight was calculated on the day the mice were killed. Data represents mean ± SD ($n = 6$ each group), *$P < 0.05$. (c) Changes in Ki67 expression in xenograft tumors were detected by IHC staining. Scale bars, 50 μm. (d) Schematic illustration of the regulation of LSCC malignant progression by the EIF4A3—hsa_circ_0001445—hsa-miR-432-5p – RGMA axis.

hsa-miR-432-5p relieved the inhibition of hsa-miR-432-5p on the expression of RGMA and upregulated the expression of RGMA, thus playing an anti-tumor effect.

Finally, we constructed xenograft tumor models of nude mice and verified that the overexpression of hsa_circ_0001445 inhibited the proliferation of LSCC cells in vivo. We admit that our research only provides one regulatory mechanism of hsa_circ_0001445 in LSCC, and other signaling methods need to be further explored.

Conclusion

In summary, we found a circRNA (hsa_circ_0001445) associated with LSCC. And we proposed a mechanism that EIF4A3 reduced the expression of hsa_circ_0001445, and hsa_circ_0001445 inhibited the proliferation and metastasis of LSCC by directly binding to hsa-miR-432-5p to attenuate the inhibitory effect of hsa-miR-432-5p on RGMA (Figure 8d). Importantly, our research suggests that hsa_circ_0001445 may be used as a potential prognostic biomarker and therapeutic target for LSCC.

Disclosure statement

No potential conflict of interest was reported by the authors.

Funding

This research is supported by grants from the National Natural Science Foundation of China (No. 81972553).

Data availability statement

All raw data that support the findings of this study are available on request from the corresponding author.

Ethics approval and consent to participate

All experimental procedures were approved by the Ethics Committee of the Second Hospital of Hebei Medical University. Tissues were obtained at the time of surgery from patients after informed consent was written by each patient.

Author contributions

Baoshan Wang and Miaomiao Yu designed all experiments; Miaomiao Yu, Huan Cao, and Jiaxue Gao performed the experiments; Miaomiao Yu, Jianwang Yang, and Tao Liu analyzed the data; Baoshan Wang and Miaomiao Yu wrote the manuscript. All authors commented on this manuscript.

References

[1] Falco M, Tammaro C, Takeuchi T, et al. Overview on molecular biomarkers for laryngeal cancer: looking for new answers to an old problem. Cancers (Basel). 2022;14:1716. doi: 10.3390/cancers14071716

[2] Sung H, Ferlay J, Siegel RL, et al. Global cancer statistics 2020: GLOBOCAN estimates of incidence and mortality worldwide for 36 cancers in 185 countries. CA Cancer J Clin. 2021;71(3):209–249. doi: 10.3322/caac.21660

[3] Steuer CE, El-Deiry M, Parks JR, et al. An update on larynx cancer. CA Cancer J Clin. 2017;67(1):31–50. doi: 10.3322/caac.21386

[4] Wu Y, Zhang Y, Zheng X, et al. Circular RNA circCORO1C promotes laryngeal squamous cell carcinoma progression by modulating the let-7c-5p/PBX3 axis. Mol Cancer. 2020;19(1):99. doi: 10.1186/s12943-020-01215-4

[5] Ludwig ML, Birkeland AC, Hoesli R, et al. Changing the paradigm: the potential for targeted therapy in laryngeal squamous cell carcinoma. Cancer Biol Med. 2016;13(1):87–100. doi: 10.20892/j.issn.2095-3941.2016.0010

[6] Cancer of the larynx—cancer stat facts. [(accessed on April 20, 2022)]; Available online: https://seer.cancer.gov/statfacts/html/laryn.html.

[7] Kristensen LS, Andersen MS, Stagsted LVW, et al. The biogenesis, biology and characterization of circular RNAs. Nat Rev Genet. 2019;20(11):675–691. doi: 10.1038/s41576-019-0158-7

[8] Memczak S, Jens M, Elefsinioti A, et al. Circular RNAs are a large class of animal RNAs with regulatory potency. Nature. 2013;495(7441):333–338. doi: 10.1038/nature11928

[9] Kristensen LS, Jakobsen T, Hager H, et al. The emerging roles of circRnas in cancer and oncology. Nat Rev Clin Oncol. 2022;19(3):188–206. doi: 10.1038/s41571-021-00585-y

[10] Lin C, Ma M, Zhang Y, et al. The N(6)-methyladenosine modification of circALG1 promotes the metastasis of colorectal cancer mediated by the miR-342-5p/PGF signalling pathway. Mol Cancer. 2022;21(1):80. doi: 10.1186/s12943-022-01560-6

[11] Pan Z, Zhao R, Li B, et al. EWSR1-induced circNEIL3 promotes glioma progression and exosome-mediated macrophage immunosuppressive polarization via

stabilizing IGF2BP3. Mol Cancer. 2022;21(1):16. doi: 10.1186/s12943-021-01485-6

[12] Duan JL, Chen W, Xie JJ, et al. A novel peptide encoded by N6-methyladenosine modified circMAP3K4 prevents apoptosis in hepatocellular carcinoma. Mol Cancer. 2022;21(1):93. doi: 10.1186/s12943-022-01537-5

[13] Song F, Yang Z, Li L, et al. MiR-552-3p promotes malignant progression of gallbladder carcinoma by reactivating the Akt/β-catenin signaling pathway due to inhibition of the tumor suppressor gene RGMA. Ann Transl Med. 2021;9(17):1374. doi: 10.21037/atm-21-2013

[14] Li Y, Wang YW, Chen X, et al. MicroRNA-4472 promotes tumor proliferation and aggressiveness in breast cancer by targeting RGMA and inducing EMT. Clin Breast Cancer. 2020;20(2):e113–e126. doi: 10.1016/j.clbc.2019.08.010

[15] Lu Y, Li Y, Wang Z, et al. Downregulation of RGMA by HIF-1A/miR-210-3p axis promotes cell proliferation in oral squamous cell carcinoma. Biomed Pharmacother. 2019;112:108608. doi: 10.1016/j.biopha.2019.108608

[16] Li S, Liu F, Zheng K, et al. CircDOCK1 promotes the tumorigenesis and cisplatin resistance of osteogenic sarcoma via the miR-339-3p/IGF1R axis. Mol Cancer. 2021;20(1):161. doi: 10.1186/s12943-021-01453-0

[17] Gui CP, Liao B, Luo CG, et al. circCHST15 is a novel prognostic biomarker that promotes clear cell renal cell carcinoma cell proliferation and metastasis through the miR-125a-5p/EIF4EBP1 axis. Mol Cancer. 2021;20(1):169. doi: 10.1186/s12943-021-01449-w

[18] Chen Q, Wang H, Li Z, et al. Circular RNA ACTN4 promotes intrahepatic cholangiocarcinoma progression by recruiting YBX1 to initiate FZD7 transcription. J Hepatol. 2022;76(1):135–147. doi: 10.1016/j.jhep.2021.08.027

[19] Yang X, Ye T, Liu H, et al. Expression profiles, biological functions and clinical significance of circRnas in bladder cancer. Mol Cancer. 2021;20(1):4. doi: 10.1186/s12943-020-01300-8

[20] Ma C, Shi T, Qu Z, et al. CircRNA_ACAP2 suppresses EMT in head and neck squamous cell carcinoma by targeting the miR-21-5p/STAT3 signaling axis. Front Oncol. 2020;10:583682. doi: 10.3389/fonc.2020.583682

[21] Gao W, Guo H, Niu M, et al. circPARD3 drives malignant progression and chemoresistance of laryngeal squamous cell carcinoma by inhibiting autophagy through the PRKCI-Akt-mTOR pathway. Mol Cancer. 2020;19(1):166. doi: 10.1186/s12943-020-01279-2

[22] Wu P, Fang X, Liu Y, et al. N6-methyladenosine modification of circCUX1 confers radioresistance of hypopharyngeal squamous cell carcinoma through caspase1 pathway. Cell Death Dis. 2021;12(4):298. doi: 10.1038/s41419-021-03558-2

[23] Liu J, Jiang X, Zou A, et al. circIGHG-Induced Epithelial-to-Mesenchymal Transition Promotes Oral Squamous Cell Carcinoma Progression via miR-142-5p/IGF2BP3 Signaling. Cancer Res. 2021;81(2):344–355. doi: 10.1158/0008-5472.CAN-20-0554

[24] Yu J, Xu QG, Wang ZG, et al. Circular RNA cSMARCA5 inhibits growth and metastasis in hepatocellular carcinoma. J Hepatol. 2018;68(6):1214–1227. doi: 10.1016/j.jhep.2018.01.012

[25] Barbagallo D, Caponnetto A, Cirnigliaro M, et al. CircSMARCA5 inhibits migration of glioblastoma multiforme cells by regulating a molecular axis involving splicing factors SRSF1/SRSF3/PTB. Int J Mol Sci. 2018;19(2):480. doi: 10.3390/ijms19020480

[26] Zhang H, Meng F, Dong S. circSMARCA5 promoted osteosarcoma cell proliferation, adhesion, migration, and invasion through a competing endogenous RNA network. Biomed Res Int. 2020;2020:2539150. doi: 10.1155/2020/2539150

[27] Conn SJ, Pillman KA, Toubia J, et al. The RNA binding protein quaking regulates formation of circRnas. Cell. 2015;160(6):1125–1134. doi: 10.1016/j.cell.2015.02.014

[28] Yang T, Shen P, Chen Q, et al. FUS-induced circRHOBTB3 facilitates cell proliferation via miR-600/NACC1 mediated autophagy response in pancreatic ductal adenocarcinoma. J Exp Clin Cancer Res. 2021;40(1):261. doi: 10.1186/s13046-021-02063-w

[29] Chen T, Wang X, Li C, et al. CircHIF1A regulated by FUS accelerates triple-negative breast cancer progression by modulating NFIB expression and translocation. Oncogene. 2021;40(15):2756–2771. doi: 10.1038/s41388-021-01739-z

[30] Ivanov A, Memczak S, Wyler E, et al. Analysis of intron sequences reveals hallmarks of circular RNA biogenesis in animals. Cell Rep. 2015;10(2):170–177. doi: 10.1016/j.celrep.2014.12.019

[31] Zheng L, Liang H, Zhang Q, et al. circPTEN1, a circular RNA generated from PTEN, suppresses cancer progression through inhibition of TGF-β/Smad signaling. Mol Cancer. 2022;21(1):41. doi: 10.1186/s12943-022-01495-y

[32] Wang G, Sun D, Li W, et al. CircRNA_100290 promotes GC cell proliferation and invasion via the miR-29b-3p/ITGA11 axis and is regulated by EIF4A3. Cancer Cell Int. 2021;21(1):324. doi: 10.1186/s12935-021-01964-2

[33] Yang M, Hu H, Wu S, et al. EIF4A3-regulated circ_0087429 can reverse EMT and inhibit the progression of cervical cancer via miR-5003-3p-dependent upregulation of OGN expression. J Exper Cli Can Res CR. 2022;41(1):165. doi: 10.1186/s13046-022-02368-4

[34] Jiang X, Guo S, Wang S, et al. EIF4A3-induced circARHGAP29 promotes aerobic glycolysis in docetaxel-resistant prostate cancer through IGF2BP2/c-Myc/LDHA signaling. Cancer Res. 2022;82(5):831–845. doi: 10.1158/0008-5472.CAN-21-2988

[35] Liu Y, Song J, Zhang H, et al. EIF4A3-induced circTOLLIP promotes the progression of hepatocellular carcinoma via the miR-516a-5p/PBX3/EMT pathway.

J Exper Cli Can Res CR. 2022;41(1):164. doi: 10.1186/s13046-022-02378-2

[36] Zhong Y, Du Y, Yang X, et al. Circular RNAs function as ceRNAs to regulate and control human cancer progression. Mol Cancer. 2018;17(1):79. doi: 10.1186/s12943-018-0827-8

[37] Tay Y, Rinn J, Pandolfi PP. The multilayered complexity of ceRNA crosstalk and competition. Nature. 2014;505(7483):344–352. doi: 10.1038/nature12986

[38] Zhang YP, Liu KL, Wang YX, et al. Down-regulated RBM5 inhibits bladder cancer cell apoptosis by initiating an miR-432-5p/β-catenin feedback loop. FASEB J. 2019;33(10):10973–10985. doi: 10.1096/fj.201900537R

[39] Yun Z, Yue M, Kang Z, et al. Reduced expression of microRNA-432-5p by DNA methyltransferase 3B leads to development of colorectal cancer through upregulation of CCND2. Exp Cell Res. 2022;410(1):112936. doi: 10.1016/j.yexcr.2021.112936